

Impedance and Thermodynamic Analysis of Bioanode, Abiotic Anode, and Riboflavin-Amended Anode in Microbial Fuel Cells

Sokhee Jung,* Young-Ho Ahn,[†] Sang-Eun Oh,[‡] Junho Lee,[§] Kyu Taek Cho,[#] Youngjin Kim, Myeong Woon Kim,[¶] Joonmok Shim,[§] and Moonsung Kang^{**}

Sustainability Consulting Group, Samsung SDS, Seoul 135-918, Korea. *E-mail: sokheejung@gmail.com

[†]School of Civil and Environmental Engineering, Yeungnam University, Gyongsan 712-749, Korea

[‡]Department of Biological Environment, Kangwon National University, Chuncheon 200-701, Korea

[§]Department of Environmental Engineering, Korea University of Transportation, Chungju 380-702, Korea

[#]Environmental Energy Technologies Division, Lawrence Berkeley National Laboratory, CA, USA

[¶]Department of Environmental Engineering, Daejin University, Pocheon 487-711, Korea

[§]Korea Institute of Energy Research, Daejeon 305-343, Korea

^{**}Department of Environmental Engineering, Sangmyung University, Cheonan 330-720, Korea

Received June 28, 2012, Accepted July 17, 2012

Understanding exoelectrogenic reactions of the bioanode is limited due to its complexity and the absence of analytics. Impedance and thermodynamics of bioanode, abiotic anode, and riboflavin-amended anode were evaluated. Activation overpotential of the bioanode was negligible compared with that of the abiotic anode. Impedance spectroscopy shows that the bioanode had much lower charge transfer resistance and higher capacitance than the abiotic anode in low frequency reaction. In high frequency reaction, the impedance parameters, however, were relatively similar between the bioanode and the abiotic anode. At open-circuit impedance spectroscopy, a high frequency arc was not detected in the abiotic anode in Nyquist plot. Addition of riboflavin induced a phase angle shift and created curvature in high-frequency arc of the abiotic anode, and it also drastically changed impedance spectra of the bioanode.

Key Words : Bioanode, Abiotic anode, Impedance, Anode biofilm, Microbial fuel cell

Introduction

Anode biofilm is a crucial component in microbial fuel cells (MFCs) for electrogenesis. The main enzymatic components for electrogenesis of anode biofilm are *exoelectrogens*, microorganisms that are capable of extracellular electron transfer.^{1,2} There have been many physical, chemical, and biological approaches to understand MFC process.³⁻⁸ However, understanding electrochemical reactions of the bioanode is limited due to its complexity and the absence of appropriate analytical methods. Improved understanding of the bioanode process is believed to enhance MFC operation and performance.

Anode biofilm formation was shown to increase power density and capacitance, and decreased charge transfer resistance. For example, development of anode biofilms considerably decreased anodic charge transfer and increased power density. They indicate anode biofilm facilitated electron transfer to the anode surface.⁹⁻¹² Initial development of anode biofilm during the first five days decreased anodic charge transfer resistance by about 40% (from 2.6 to 1.5 kΩ cm² at 0.27 A/m²) in a ferricyanide-cathode MFC, with increasing power density by about 120%.¹¹ Anodic charge transfer resistance decreased by ~75% (from 0.073 to 0.017 kΩ cm² at 2.63 A/m²) in an air-cathode MFC, with increasing anodic capacitance during 70-day biofilm enrichment.¹² However, previous studies did not compare bioanode elec-

trochemistry with that of abiotic anode, which is a suitable baseline for accurate evaluation.

Riboflavin, also known as vitamin B2 (C₁₇H₂₀N₄O₆), plays a key role in energy metabolism. Flavin mononucleotide (riboflavin-5-phosphate) is a biomolecule made from riboflavin *via* riboflavin kinase activity, and it functions as prosthetic group of various oxidoreductases including NADH dehydrogenase. *Shewanella* species secretes flavins to perform exoelectrogenesis¹³ in the subsurface or the MFC condition. In an MFC experiment of *S. oneidensis* MR-1 and MR-4, more than 70% of electron transfer accounted for flavin mediation. Though riboflavin is very important in mediator-driven bioelectricity generation, their role on electron transfer resistance has not been precisely investigated yet.

Electrochemical impedance spectroscopy (EIS) is an attractive technique to study anode electrochemistry; application of EIS does not sacrifice anode electrode and yields quantitative values of anode electrochemical process.¹⁴⁻¹⁶ With the importance of pH on bioenergy processes,¹⁷ in a recent study of pH effects on the bioanode process,¹⁴ resistance, capacitance, and nonideality constants of two charge transfer reactions were accurately differentiated and quantified using the equivalent circuit model BIOANODE-1, which was used to analyze anode impedance in this study.

We compared impedance and thermodynamics of a bioanode with an abiotic anode to test electrochemical property

of the anode biofilm, and also investigated effects of riboflavin on electron transfer using EIS. Impedance parameters of various anodes were characterized using charge transfer resistance, capacitance, and nonideality constants. Thermodynamics were evaluated using anode polarization by modulating poised anode potential. Overall, this study will increase understanding the bioanode electrochemistry.

Experimental

MFC Construction and Operation. Single-chambered MFCs (250 mL)¹⁸ were used with a carbon cloth anode (2.5 cm × 6 cm, 30 cm², BASF Fuel Cell Inc., Somerset, NJ; CC-A) and an air cathode (7 cm² of Pt-coated area, four PTFE diffusion layers on a 30 wt % wet-proofed carbon cloth type B-1B, E-TEK) by applying platinum (0.5 mg Pt/cm²) on one side (Fig. 1). Ag/AgCl reference electrodes (BASi MF-2079, IN) were inserted through a rubber stopper in a sidearm sampling port and sealed using silicon glue.

Phosphate-buffer medium (50 mM, pH 7) containing trace elements (10 mL/L) and vitamins (10 mL/L) was used with amendment of acetic acid (10 mM) for electron donor.¹⁹ Suspension (100 mL) from an electricity-producing acetate-fed MFC was used to inoculate anode electrode for the bioanode test, however, the abiotic anode was not inoculated. The circuit was connected with 460-Ω resistance in the acclimation step (10 days) and 100-Ω resistance thereafter (an additional 20 days). Riboflavin (MW 376.36, 98%, CAS# 63-88-5, Alfa Aesar) was added at a final concentration of 1 mM to test the effect of exogenous redox mediator.

Anode EIS Analysis. EIS was performed using a potentiostat Reference 600 (Gamry Instrument Inc.) in a fresh medium condition. Anodes were poised at each test potential

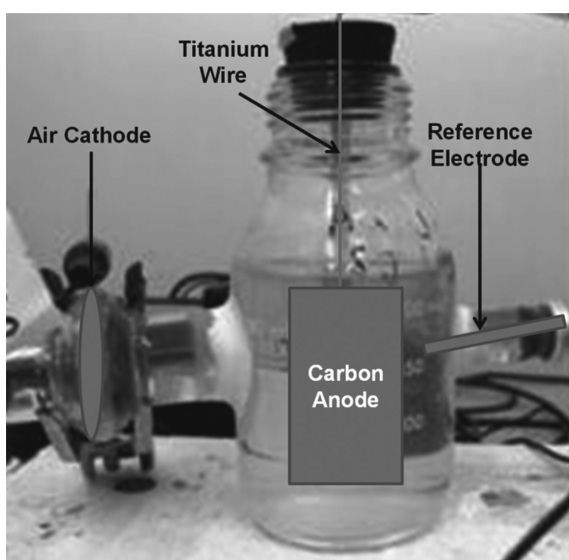


Figure 1. Single-chambered MFC used in this experiment. Positions of air cathode, carbon anode, titanium wire, and reference electrode were indicated by drawings because cloudy medium in the reactor lowered their visibility.

for 30 minutes, and EIS was performed at each potential with the following conditions: AC potential 10 mV rms,

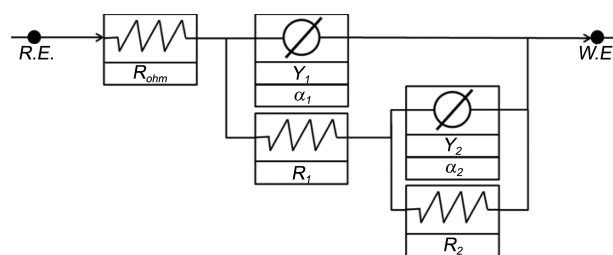


Figure 2. Equivalent circuit BIOANODE-1¹⁴ used in this study. It models two sequential charge transfer reactions in the bioanode. R.E. is reference electrode, W.E. is working electrode, R_{ohm} is ohmic resistance, Y is admittance, and a is nonideality constant. Subscript number 1 is associated with a charge transfer reaction detected in high frequency, and number 2 is associated with that in low frequency.

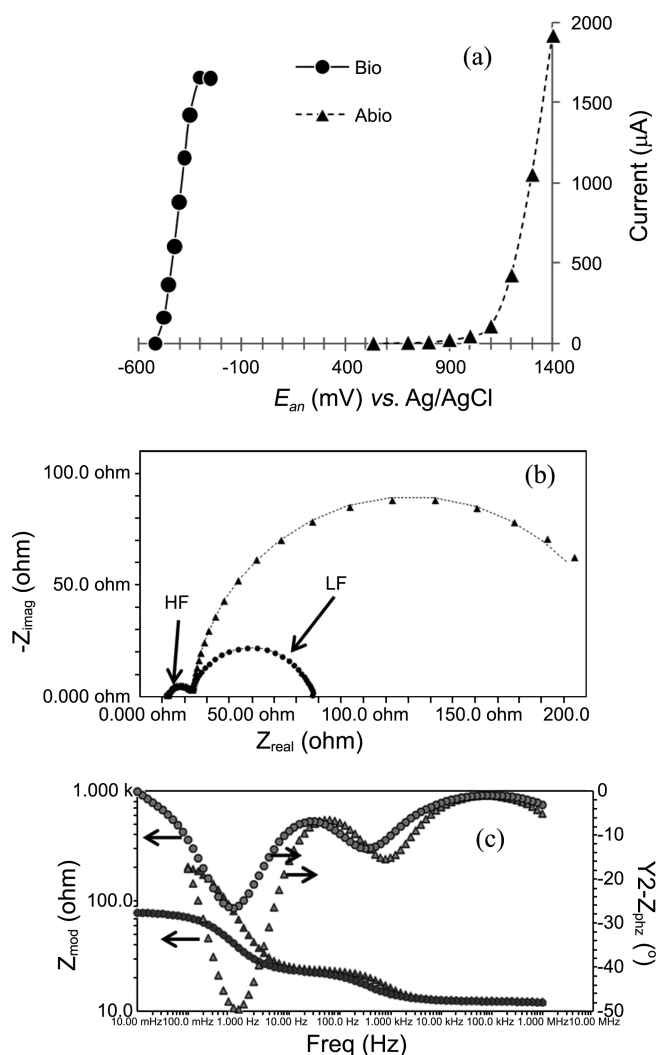


Figure 3. Anode polarization curves (a), Nyquist plots (b), and Bode plots (c). Current values after 30 minutes at each poised potential were used for anode polarization curves. Nyquist plots (b) and Bode plots (c) were measured when the bioanode (Bio) was poised at 0.37 mA (−0.45 V) and the abiotic anode (Abio) was poised at 0.42 mA (1.2 V). (LF: low frequency, HF: high frequency).

initial frequency 10^6 or 10^5 Hz, final frequency 50 or 10 mHz, and 10 points/decade of data acquisition frequency.

Impedance spectra were fitted with BIOANODE-1 by χ^2 -minimization using Echem Analyst (Gamry Instrument Inc.) (Fig. 2). Equivalent circuit model BIOANODE-1 is composed of two successive RC time constants, where an arc detected in low frequency domain is associated with initiating reactions for bioelectricity generation (R_2 , C_2 and α_2) and an arc detected in high frequency domain is associated with the electron transfer reaction (R_1 , C_1 and α_1).¹⁴

Resistance (R) is the property that resists a steady current flow. Capacitance (C) is the ability of electrical bodies to hold electrical charges. The nonideality constant (α) is a measure of how electrical circuit behaves differently from

the ideal circuit. A constant phase element (CPE) was incorporated to model a non-ideal capacitor of MFC anode, defined as $1/Z = Y(j\omega)^\alpha$, where $Y(S \cdot s^\alpha)$ is a numerical value of the admittance ($1/|Z|$) at $\omega = 1$, α is an empirical non-ideality constant, $j = \sqrt{-1}$, and ω (s^{-1}) is the radial frequency ($\omega = 2\pi f$).²⁰ Capacitance (C) was calculated using $C = (YR_p)^{1/\alpha}/R_p$, where R_p (Ω) is the charge transfer resistance.²⁰

Calculations. Redox potential (or reduction potential) in a hypothetical condition at pH 7 and 303 K (30 °C) was calculated using the Nernst equation as previously described.¹⁴ By applying the obtained R_p from EIS, the exchange current (i^0) was calculated using the Tafel equation $R_p = RT/nF i^0$, where n is the number of electrons involved in the reaction (8 for complete acetate oxidation).^{21,22} Potential values were

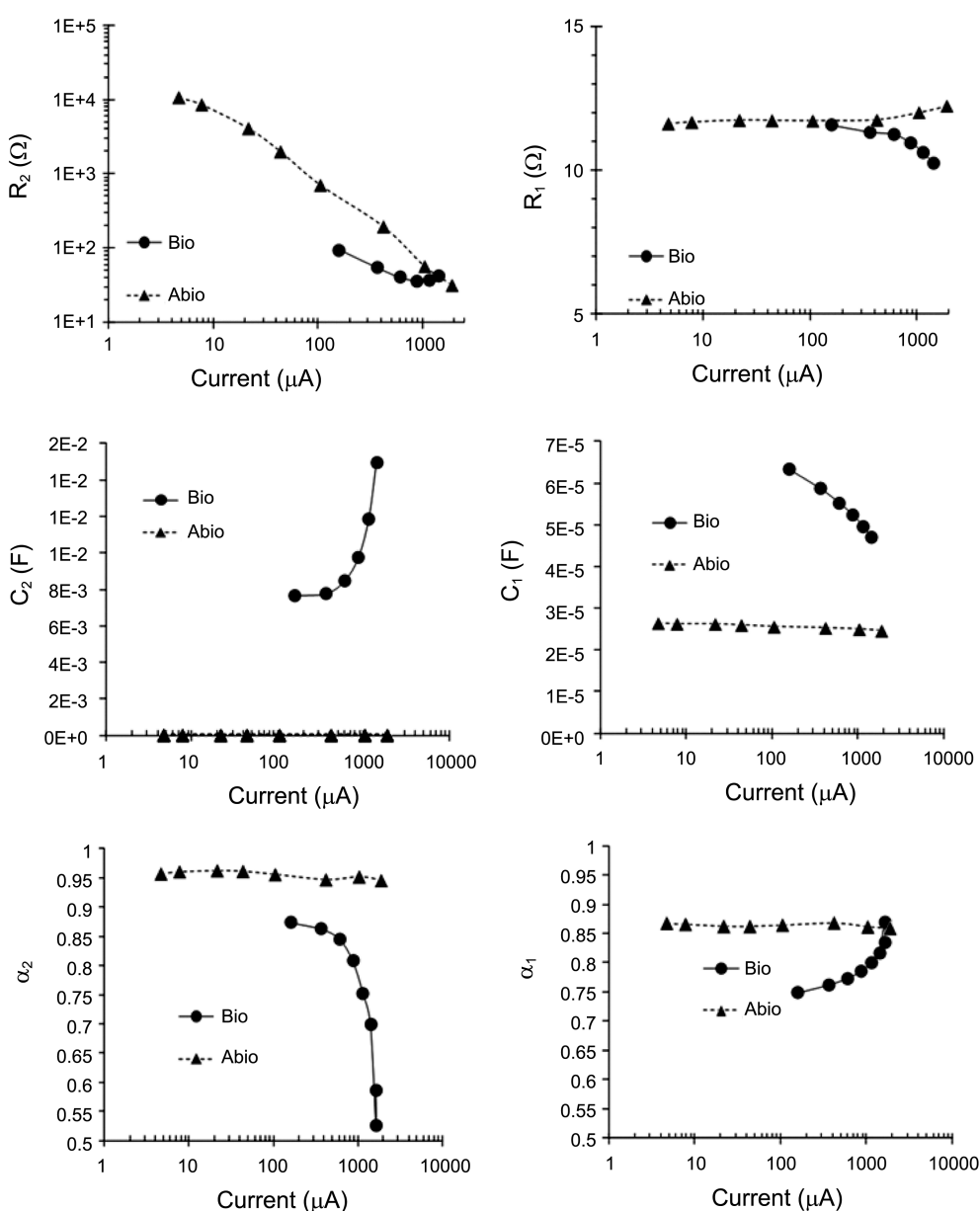


Figure 4. Impedance parameters variations upon the current change. Transitions of charge transfer resistance (R), capacitance (C), and nonideality constant (α) with respect to current development in the bionanode (Bio) and the abiotic anode (Abio). Impedance parameters (R_2 , C_2 , and α_2) in a left column are related to low frequency reaction in the Nyquist plot, and impedance parameters (R_1 , C_1 , and α_1) in a right column are related to high frequency reaction.

reported with respect to Ag/AgCl using the equation of Ag/AgCl = SHE - 197 mV.²³

Results and Discussion

Impact of Anode Biofilm on Activation Overpotential.

The Bioanode had negligible activation overpotential than that of the abiotic anode. Open circuit potentials (OCPs) were 533 mV for the abiotic anode and -516 mV for the bioanode, and their difference was 1049 mV at open circuit ($i \approx 0$) (Fig. 3). Potential difference increased up to ~1700 mV as current produced more than 100 μA , mainly due to the ~600 mV of activation overpotential in the abiotic anode (Fig. 3). At pH 7 and 303 K, acetate oxidation has a potential of -503 mV at the initial batch conditions of 5 mM of HCO_3^- and 10 mM of CH_3COO^- used in these experiments, and water electrolysis has a potential of 585 mV assuming 10% of O_2 saturation (0.02 mM) at 30 °C. Measured OCPs of the bioanode (-516 mV) and the abiotic anode (533 mV) were close to the above thermodynamic, which was similar to a previous foundation.¹⁴ When acetate was not added in the abiotic anode system, anodic polarization behaviors and impedance spectra were almost identical to the acetate-added system (data not shown).

Although water hydrolysis ($E = 585$ mV) needs 1.088 V more potential energy than acetate oxidation ($E = -503$ mV), water was preferentially used as an electron donor in the abiotic anode even in the presence of acetate (10 mM). Our results demonstrate acetate is not oxidized in the absence of anode biofilm, but rather only water electrolysis occurs at a high anode potential (Fig. 3). Because catalyst is a substance changing the rate of a chemical reaction, it implies anode biofilm might not be called a catalyst.

In the abiotic anode, a huge activation potential (~600 mV) was detected. Activation overpotential is caused by the slowness of the reaction occurring on the electrode surface.²² Activation overpotential can be minimized by more effective catalyst, increasing surface area, or high temperature in chemical fuel cells.²² Anode biofilm formation made the acetate oxidation possible and made activation overpotential negligible when it comes to the acetate oxidation.

Impact of Anode Biofilm on Impedance. In the low frequency reaction, the bioanode had lower charge transfer resistance and higher capacitance than the abiotic anode, and the bioanode showed more non-ideal capacitance in both charge transfer processes (Fig. 4). In the bioanode, R_2 ranged from 36 to 93 Ω , C_2 ranged from 7.6 to 14.9 mF, and α_2 ranged from 0.70 to 0.87 within current range of 160 and 1424 μA . In the abiotic anode, R_2 ranged from 32 to 10680 Ω , C_2 ranged from 2.7 to 3.1 mF, and α_2 ranged from 0.95 to 0.96 within current range of 5 and 1915 μA . The impedance characteristics for the high frequency reaction were relatively similar between the abiotic anode and the bioanode. In the abiotic anode, R_1 ranged from 11.6 to 12.2 Ω , C_1 ranged from 0.025 to 0.026 mF, and α_1 ranged from 0.86 to 0.87 within current range of 5 and 1915 μA . In the bioanode, R_1 ranged from 10.3 to 11.6 Ω , C_1 ranged from 0.047 to 0.063

mF, and α_1 ranged from 0.75 to 0.82 within current range of 160 and 1424 μA .

The presence of the anode biofilm increased capacitance due to its properties as a charge storage body or conductive matrix.^{3,6,8} Charge double layer is a build-up of charges between an electrode and its surrounding electrolyte.²² The feasibility of electrochemical reactions depends on the charge densities in the charge double layer.²² Effective catalysts increase both the accumulation of charges and the probability of a reaction. In this study, total average capacitances (~30 mF) of the bioanode was 10-fold larger than the abiotic anode (~3 mF), possibly due to the dominance of *Geobacter sulfurreducens*. *G. sulfurreducens* is a dominant exoelectrogenic strain of the anode biofilm in this tested MFC system.^{1,7,19,24-27} Because *G. sulfurreducens* utilize acetyl-CoA transferase or acetate kinase coupled with phosphate transacetylase to initially activate acetate into acetyl-CoA for the sequential central metabolism,²⁸ acetate could be utilized as an electron donor preferentially and activation overpotential also could be minimized.

Except for the linear decrease of R_2 with increasing current, other impedance parameters of the abiotic anode were relatively constant over the tested current range (Fig. 4). On the other hand, impedance parameters changed during current development in the bioanode. Total impedance decreased as current increased in the abiotic anode. However, it rapidly increased without any increase of current production in the bioanode (Fig. 5).

Effects of Riboflavin on Bioanode Electrochemistry. At open circuit, the abiotic anode did not have a high-frequency arc in Nyquist plot (Fig. 6). Addition of riboflavin (1 mM) mainly affected the high frequency impedance of the abiotic anode and the low frequency impedance of the bioanode. In the abiotic anode, riboflavin induced a phase angle shift and created curvature in the high frequency impedance in Nyquist plots (Fig. 6(a) and (b)).

In the bioanode, riboflavin addition drastically reduced

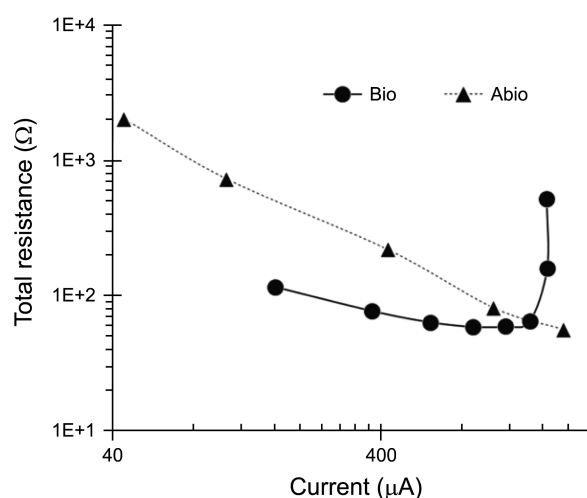


Figure 5. Total Resistance of anodes upon the current change. Sum of total charge transfer and diffusion resistance in the bioanode (Bio) and the abiotic anode (Abio) were shown with respect to current development.

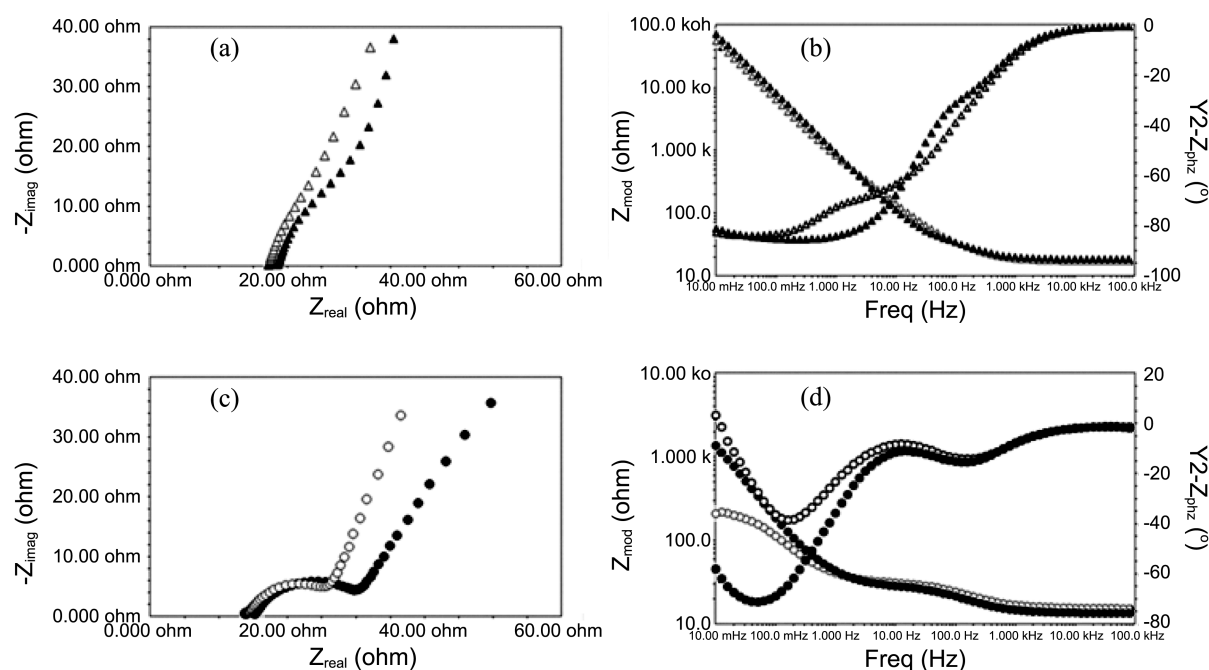


Figure 6. Impedance spectra from the abiotic anode (a and b) and the bioanode (c and d) measured at open circuit. A and C are Nyquist plots, and B and D are Bode plots. Closed symbols represent impedance spectra when 1 mM of riboflavin was added.

R_2 from 531 to 162 Ω , increased C_2 from 7.2 to 10.0 mF, and decreased α_2 from 0.97 to 0.92 (Fig. 6(c) and (d)). The effects of riboflavin addition on the high frequency reaction were less pronounced; it increased R_1 from 14.0 to 15.1 Ω , decreased C_1 from 0.53 to 0.25 mF, decreased α from 0.79 to 0.72 (Fig. 4(c) and (d)). Exchange current (i^0) increased from 0.6×10^{-2} to 1.8×10^{-2} mA when riboflavin was added.

Shewanella species secrete flavins such as riboflavin and FMN to perform exoelectrogenesis.¹³ It was shown that *Shewanella* species utilized riboflavin as an electron transfer mediator in MFC condition.²⁹ In order to create a distinguishable effect of riboflavin, high riboflavin concentration (1 mM) was applied in this research. The phase angle shift and curvature occurrence in high frequency were shown when riboflavin was added to the abiotic anode, indicating riboflavin might activate the high frequency reaction.

In the bioanode, riboflavin addition increased charge storage and charge transfer in the low frequency reaction, which was demonstrated by the changes of capacitance and charge transfer resistance. Exchange current calculated from the Tafel equation increased three times, and it shows that activation overpotential decreased by several orders of magnitude.^{22,30} These results also show riboflavin might increase exoelectrogenic microbial activity because the low frequency reaction was suggested to be intracellular microbial activity¹⁴ and because electron transfer mediator was increased by adding riboflavin.

Conclusion

The bioanode had negligible activation overpotential. The

bioanode had lower charge transfer resistance and higher capacitance for the low frequency reaction than the abiotic anode, and it showed more non-ideal capacitance in both charge transfer processes. In the abiotic anode, riboflavin induced a phase angle shift and created curvature in the high frequency arc in Nyquist plots. In the bioanode, riboflavin addition increased capacitance and charge transfer. For future work, anode community analysis upon riboflavin addition would show what microbial groups would be dominant in the redox-shuttle-driven exoelectrogenic condition.

Acknowledgments. The authors thank Dr. John M. Regan (Associate Professor, Department of Civil and Environmental Engineering, Penn State University) for his support. This research was supported by Scholarship from Korean-American Scientists and Engineers Association (KSEA).

References

- Jung, S.; Regan, J. M. *Appl. Environ. Microbiol.* **2011**, *77*, 564.
- Logan, B. E.; Regan, J. M. *Trends in Microbiology* **2006**, *14*, 512.
- Marcus, A. K.; Torres, C. I.; Rittmann, B. E. *Biotechnol. Bioeng.* **2007**, *98*, 1171.
- Pham, T. H.; Aelterman, P.; Verstraete, W. *Trends in Biotechnology* **2009**, *27*, 168.
- Torres, C. I.; Marcus, A. K.; Lee, H. S.; Parameswaran, P.; Krajmalnik-Brown, R.; Rittmann, B. E. *FEMS Microbiology Reviews* **2010**, *34*, 3.
- Ha, P. T.; Moon, H.; Kim, B. H.; Ng, H. Y.; Chang, I. S. *Biosens. Bioelectron.* **2010**, *25*, 1629.
- Wang, X.; Feng, Y.; Ren, N.; Wang, H.; Lee, H.; Li, N.; Zhao, Q. *Electrochimica Acta* **2009**, *54*, 1109.
- Hong, Y.; Call, D. F.; Werner, C. M.; Logan, B. E. *Biosens. Bio-*

- electron*. **2011**, 28, 71.
9. Manohar, A. K.; Bretschger, O.; Nealon, K. H.; Mansfeld, F. *Electrochimica Acta* **2008**, 53, 3508.
10. Marsili, E.; Rollefson, J. B.; Baron, D. B.; Hozalski, R. M.; Bond, D. R. *Appl. Environ. Microbiol.* **2008**, 74, 7329.
11. Ramasamy, R. P.; Ren, Z. Y.; Mench, M. M.; Regan, J. M. *Biotechnol. Bioeng.* **2008**, 101, 101.
12. Borole, A. P.; Aaron, D.; Hamilton, C. Y.; Tsouris, C. *Environ. Sci. Technol.* **2010**, 44, 2740.
13. von Canstein, H.; Ogawa, J.; Shimizu, S.; Lloyd, J. R. *Appl. Environ. Microbiol.* **2008**, 74, 615.
14. Jung, S.; Mench, M. M.; Regan, J. M. *Environ. Sci. Technol.* **2011**, 45, 9069.
15. He, Z.; Mansfeld, F. *Energy & Environmental Science* **2009**, 2, 215.
16. Ouitrakul, S.; Sriyudthsak, M.; Charojrochkul, S.; Kakizono, T. *Biosens. Bioelectron.* **2007**, 23, 721.
17. Cheng, C.-H.; Hung, C.-H.; Lee, K.-S.; Liao, P.-Y.; Liang, C.-M.; Yang, L.-H.; Lin, P.-J.; Lin, C.-Y. *Inter. J. Hydrogen Energy* **2008**, 33, 5242.
18. Logan, B.; Cheng, S.; Watson, V.; Estadt, G. *Environ. Sci. Technol.* **2007**, 41, 3341.
19. Jung, S.; Regan, J. M. *Appl. Microbiol. Biotechnol.* **2007**, 77, 393.
20. Macdonald, J. R. *Ann. Biomed. Eng.* **1992**, 20, 289.
21. Wagner, N. J. *Appl. Electrochem.* **2002**, 32, 859.
22. Larminie, J.; Dicks, A. *Fuel Cell System Explained*; Wiley: West Sussex, 2002.
23. Bard, A.; Faulkner, L. *Electrochemical Methods: Fundamentals and Applications*; John Wiley & Sons: 2001.
24. Xing, D.; Cheng, S.; Regan, J. M.; Logan, B. E. *Biosens. Bioelectron.* **2009**, 25, 105.
25. Bond, D. R.; Holmes, D. E.; Tender, L. M.; Lovley, D. R. *Science* **2002**, 295, 483.
26. Lee, H.-S.; Parameswaran, P.; Kato-Marcus, A.; Torres, C. I.; Rittmann, B. E. *Water Res.* **2008**, 42, 1501.
27. Logan, B. E. *Nat. Rev. Micro.* **2009**, 7, 375.
28. Mahadevan, R.; Bond, D. R.; Butler, J. E.; Esteve-Nunez, A.; Coppi, M. V.; Palsson, B. O.; Schilling, C. H.; Lovley, D. R. *Appl. Environ. Microbiol.* **2006**, 72, 1558.
29. Marsili, E.; Baron, D. B.; Shikhare, I. D.; Coursolle, D.; Gralnick, J. A.; Bond, D. R. *Proc. Natl. Acad. Sci. USA* **2008**, 105, 3968.
30. Mench, M. M. *Fuel Cell Engines*; John Wiley and Sons, Inc.: New York, 2008.
-